Mechanisms of Influenza Virus HA2 Peptide Interaction with Liposomes Studied by Dual-Wavelength MP-SPR

Meryem Belkilani, Carole Farre, Yves Chevalier, Sylvain Minot, François Bessueille, Adnane Abdelghani, Nicole Jaffrezic-Renault, Carole Chaix

Mechanisms of Influenza virus HA2 peptide interaction with liposomes studied by dual-wavelength MP-SPR

Meryem Belkilani,[†,‡,§] *Carole Farre,*[†] *Yves Chevalier,*[#] *Sylvain Minot,*[†] *François Bessueille,*[†] *Adnane Abdelghani,*[§] *Nicole Jaffrezic-Renault,*[†] *Carole Chaix*[†*]

[†]University of Lyon, CNRS, Claude Bernard Lyon 1 University, Institute of Analytical Sciences, 5 rue de la Doua, F-69100 Villeurbanne, France.

[‡] University of Tunis, ENSIT, av. Taha Hussein, Montfleury, 1008 Tunis, Tunisia.

[§] University of Carthage, INSAT, Research Unit of Nanobiotechnology and Valorisation of Medicinal Plants, 1080 Charguia Cedex, Tunisia.

[#] University of Lyon, CNRS, Claude Bernard Lyon 1 University, LAGEPP, 43 bd 11 Novembre, F-69622 Villeurbanne, France.

[*] Corresponding authors: carole.chaix-bauvais@univ-lyon1.fr

KEYWORDS. Multi-parametric surface plasmon resonance (MP-SPR), Liposome, Streptavidin, HA2 peptide, Phospholipid, Influenza virus.

ABSTRACT

A phospholipid-based liposome layer was used as an effective biomimetic membrane model to study the binding of the pH-dependent fusogenic peptide (E4-GGYC) from the Influenza virus hemagglutinin HA2 subunit. To this end, a multi-parameter surface plasmon resonance approach (MP-SPR) was used for monitoring peptide-liposome interactions at two pH values (4.5 and 8) by means of recording sensorgrams in real-time without the need for labeling. Biotinylated liposomes were firstly immobilized as a monolayer onto the surface of a SPR gold chip coated with a streptavidin layer. Multiple sets of sensorgrams with different HA2 peptide concentrations were generated at both pHs. Dual-wavelength Fresnel layer modeling was applied to calculate the thickness (*d*) and the refractive index (*n*) of the liposome layer in order to monitor the change in its optical parameters upon interaction with the peptide. At acidic pH, the peptide, in its alpha helix form, entered the lipid bilayer of liposomes, inducing vesicle swelling and increasing membrane robustness. Conversely, a contraction of liposomes was observed at pH 8, associated with non-insertion of the peptide in the double layer of phospholipids. The equilibrium dissociation constant $K_D = 4.7 \times 10^{-7}$ M of the peptide/liposome interaction at pH 4.5 was determined by fitting the "OneToOne" model to the experimental sensorgrams using Trace Drawer™ software. Our experimental approach showed that the HA2 peptide at a concentration up to 100 µM produced no disruption of liposomes at pH 4.5.

INTRODUCTION

Surfaces coated with liposomes are excellent biomimetic systems as their structure is similar to cell membranes and other biological barriers mostly consisting of phospholipids. We have used herein these functional surfaces to study their interaction with HA2 peptide. The HA2 peptide is a 20 amino acid sequence derived from the N-extremity of the second hemagglutinin subunit (HA2) of the Influenza virus.[1] Here, we studied the HA2 peptide with a glutamic acid-substituted glycine at position 4 of the wild-type sequence. A stronger pH-dependence of its membrane-penetrating properties has been shown with this variant.[1,2] The peptide was found to insert into the phospholipid bilayer only at acidic pH. The COOH end was also modified by adding GGYC amino acids as described in a previous work.[3] The HA2 peptide variant is referred to as E4-GGYC throughout this paper. During infection, the hemagglutinin of the Influenza virus operates structural rearrangements through acidification (pH ≤ 6), which allow its N-terminal fusogenic sequence to enter the target endosomal membrane.[4] Structural studies carried out on the HA2 peptide have shown that it adopts an α-helical conformation to trigger fusion. [5] The three glutamic acids and one aspartic acid residues of the E4-variant are protonated at low pH, inducing a conformation change to a rigid α-helix conformation.[2,6] Luneberg *et al.* studied the interaction mechanism of the HA2 peptide with phosphatidylcholine liposomes as model membrane.[7] The fusogenic properties of the HA2 peptide mainly results from the amphipathic structure of the α-helix, all glycines of the sequence being located on one side of the helix, whereas the bulky hydrophobic residues are found at the opposite side of the helix.[7] They found an oblique insertion of the peptide into the lipid bilayer with an angle of about 45 ° between the helix axis and the membrane plane using FTIR spectroscopy. This angle was 30 ° from theoretical calculations in another reference.[8] The interaction of the AcE4K analog of HA2 peptide with 1-stearoyl-2-oleoyl phosphatidylcholine liposomes was also investigated by Zhelev *et al.*[6] They showed the pH-dependent partitioning in the membrane and the reversibility

of the binding, by circular dichroism and fluorescence experiments. They also hypothesized the formation of pores within the membrane at low pH (pH 4.0–4.5), which could cause the leakage of internalized solutes.[6] The membrane-disrupting properties of HA2 peptide was studied by a liposome leakage assay based on the release of calcein encapsulated inside the vesicles.[2] The peptide caused such leakage only at acidic pH, between 4.0 and 6.5. This active peptide with regard to the cell membrane was used to develop new therapeutic approaches. HA2 peptide-polylysine conjugate was developed as a gene-transfer vehicle.[2] The conjugate was shown to package nucleic acids as a vector that can be released from the endosome under the acidification process. This peptide was also bound on the surface of an oil-in-water nanoemulsion to facilitate transfection and endosome release.[3]

In recent years, several research papers have been devoted to the study of the mechanisms of interaction between various types of peptides and either lipid bilayers [9-12] or intact liposome layers [13-15] supported on solid substrates. These studies were monitored by surface plasmon resonance (SPR), an optical technique based on evanescent waves. SPR is a labeling-free technique suitable for real-time monitoring of interactions between lipid layers bound to the SPR chip surface and their partners in solution (i.e. peptides), providing an estimation of binding affinity and kinetic constants. The thickness (*d*) and the mean refractive index (*n*) of the layers deposited on the substrate can also be extracted from the MP-SPR signal through the optical modeling of the full angular spectra.[16-18] These parameters allow a clear description of the layers before and after the interaction with peptides.

Here, we report the monitoring of E4-GGYC interactions with a liposome-supported substrate using a dual-wavelength multi-parameter surface plasmon resonance (MP-SPR) approach based on the Kretschmann configuration. This biomimetic surface elaborated with preformed liposomes (average diameter < 100 nm) is well suited to study the specific interactions with

biomolecules. In a previous work, the rupture of liposomes by interaction with mono-rhamnolipid, an amphiphilic biomolecule, was characterized by MP-SPR.[19]

In this study, several sets of SPR sensorgrams were collected with different concentrations of E4-GGYC interacting with liposome-coated surfaces at pH 4.5 and pH 8 so as to investigate their dynamic interactions expressed in terms of the association rate constant (k_a), dissociation rate constant (k_d) and equilibrium dissociation constant (K_D). The SPR angular spectra calculated using the dual-wavelength Fresnel-layer modeling with Layer Solver™ software were fitted to the experimental sensorgrams to estimate the kinetic variation of the thickness (d) and in the refractive index (n) of the liposome layer.

Complementary information pertaining to interactions between liposomes and E4-GGYC in 3D solution was obtained from Dynamic Light Scattering (DLS) and NanoSight (Nanoparticle-Tracking Analysis, NTA).

MATERIALS AND METHODS

Chemicals. Hydrogenated soybean phosphatidylcholine HSPC (Phospholipon 90 H) was a generous gift of Lipoid company, 1,2-distearoyl-*sn*-glycero-3-phosphoethanolamine-N-[biotinyl(polyethylene glycol)-2000] (DSPE-PEG), cholesterol (99 %), 11-mercaptoundecanoic acid (MUA), 11-amino-1-undecanethiol hydrochloride, 1-dodecanethiol, streptavidin, 1-(3-dimethylaminopropyl)-3-ethylcarbodiimide (EDC), N-hydroxysuccinimide (NHS), ethanolamine, Triton X-100, NaCl, sodium dihydrogen phosphate (NaH_2PO_4), disodium hydrogen phosphate (Na_2HPO_4), tris(hydroxymethyl)aminomethane and mono-rhamnolipid (mono-RL) R95Md (95 % pure rhamnolipids, mono-rhamnolipid dominant) produced by AGAE Technologies LLC (USA) were purchased from Sigma-Aldrich. Chloroform (99.8 %) was from Fisher Chemical, diethyl ether was from Carlo Erba, methanol was from VWR company, and 2-(N-morpholino)ethanesulfonic acid (MES) was from

Dominique Dutcher company. Ultrapure water was obtained using a Milli-Q system (resistivity = 18.2 MΩ·cm).

The peptide sequence E4-GGYC was purchased from BioMérieux company. This variant was described by Wagner *et al.* [2] as a highly pH-sensitive membrane-interacting peptide. Its sequence derived from the N-end of the second hemagglutinin subunit (HA2) of the Influenza virus was NH_2-GLFEAIAGFIENGWEGMIDGGGYC-COOH (molar mass = 2506.8 g/mol). The E4-GGYC purity was 75 % based on HPLC analysis (see Figure S1 in supporting information). The peptide concentration was determined using UV-Vis absorbance (Varian CARY100 Bio) at 280 nm in pH 7 PBS buffer, using the extinction coefficient ε = 6990 (1/M.cm). All experiments were carried out using freshly prepared solutions.

Preparation of biotinylated liposomes. Biotinylated liposomes were prepared using the Bangham's "thin layer rehydration" technique [20] and a slightly modified protocol from that developed by Zhao *et al*. [21] for the preparation of small (< 100 nm) liposomes. HSPC, DSPE-PEG and cholesterol (610.8 mg, 9.8 mg and 200 mg respectively) were dissolved in 75 mL of a mixed organic solvent: chloroform, diethyl ether and methanol (5.75:5.75:1 v/v). The amount of biotinylated phospholipids was 1.5 wt % of the total phospholipids. Organic solvents were then evaporated under a reduced pressure of 0.05 MPa in a water bath at 50 °C for 3 hrs using a rotary evaporator (Buchi Rotavapor R-114 with Heating Waterbath B-480 & Glassware-Acomertial). The thin transparent layer in the round bottom flask was hydrated with 25 mL of water at 60 °C by rotating the container for 1 h until the thin layer was completely dispersed in water and a milky suspension was obtained. In order to obtain a homogeneous mixture and reduce the average size of the liposomes, the solution was sonicated for 20 min with a UP400S ultrasound device (Hielscher – Ultrasound Technology Company) at 60 kHz in an ice bath.

Biotinylated liposome characterizations. Hydrodynamic diameters of the liposomes before and after their interaction with E4-GGYC in solution were measured at 25 °C using two methods:

- Dynamic Light Scattering (DLS) with a Zetasizer NanoZS instrument (Malvern Panalytical, Palaiseau, France) operating in backscattering mode at an angle of 173 °. A disposable polystyrene cuvette was filled with 3 mL of a diluted liposome suspension (1:10) in a 0.15 M NaCl solution and in PBS buffers (0.1 M NaH_2PO_4, 0.05 M NaCl, pH 4.5) and (0.1 M Na_2HPO_4, 0.05 M NaCl, pH 8). Diameters were calculated based on the intensity distribution of data; they were given as average hydrodynamic diameters ± standard deviation (*SD*) from three independent measurements with a polydispersity index (*PdI*).

- NanoSight NS300 (Malvern Instruments Ltd, Malvern, UK), equipped with a NS300 flow-cell top plate and a laser diode operating at 405 nm. The data were analyzed using NanoSight Nanoparticle-Tracking Analysis NTA 3.4 Build 3.4.003 software. Liposomes were diluted 2.5×10^5-fold in PBS due to the relatively low particle concentrations that are required for NTA measurements (10^8–10^9 liposomes/mL).[22] 500 µL of the liposome solution was incubated with 500 µL of peptide at the final concentrations of 0, 0.5, 2, 5, 7, 10, 25, 50, 75 and 100 µM in PBS at pH 4.5 or pH 8, for 30 min at room temperature. Afterward, 1 mL of each sample was injected into the viewing chamber with a 1 mL syringe. The temperature was maintained at 25 °C. For each measurement, three 30 s videos were captured by a sCMOS camera level of 16 and analyzed by NanoSight NTA Software. The liposome sizes were expressed as the calculated means ± standard deviation (*SD*) of size distribution.

The surface potential of the liposomes was determined by ζ-potential measurements using a NanoZS Zetasizer instrument (Malvern Panalytical). The measurements were carried out in folded capillary cells DTS 1070 (Malvern Instruments) filled with 800 µL of a diluted liposome

suspension (1:10) in 0.15 M NaCl solution, PBS at pH 4.5 and pH 8, and equilibrated at 25 °C for 60 s.

SPR gold chip surface preparation. The SPR gold chips were obtained from BioNavis (BioNavis Ltd., Ylöjärvi, Finland). They are composed of a glass plate, 240 mm^2 in surface area coated with a 3 nm-thick Cr adhesive layer and a 50 nm-thick gold layer. To remove surface contamination, the SPR gold chips were cleaned before use by a microwave induced plasma (UHP-MW-PC, Diener electronic company, Stuttgard, Germany). Then, the slides were sonicated for 5 min in acetone and next in ultrapure water.

In order to form a dense self-assembled monolayer (SAM) on the gold surface, the Au substrates were dried under a nitrogen flow and immediately immersed in a 1 mM ethanolic solution of 11-mercaptoundecanoic acid (MUA) (acidic SAM), 11-amino-1-undecanethiol hydrochloride (amino SAM), or 1-dodecanethiol (alkyl SAM) for 20 hrs at 4 °C. The chips were then rinsed with ethanol and dried under a gentle nitrogen flow. SPR gold chips functionalized with the different SAMs were stored in an ultrapure water bath and used directly for liposome immobilization.

The streptavidin-coated SPR chip was prepared by derivation of the MUA chip. The latter was incubated in 100 µL of a mixture of 0.2 M EDC and 0.05 M NHS in MES buffer (5 mM MES, pH 5) for 2 hrs at room temperature to activate the carboxylic groups. The activated surfaces were washed in 1 mL of MES buffer and then incubated in 100 µL of a streptavidin solution (1 mg/mL) in PBS (0.1 M NaH_2PO_4/ Na_2HPO_4, 0.15 M NaCl, pH 7) for 12 hrs at room temperature. Afterwards, the SPR chip surfaces were rinsed with 1 mL of MES buffer, incubated in 100 µL of 10 mM tris(hydroxymethyl)aminomethane (pH = 8.1) or 10 mM 3-dimethylaminopropylamine (pH = 10.0) or 10 mM lysine (pH = 10.5) aqueous solutions for 30 min in order to deactivate all the residual active sites possibly responsible for non-specific binding, and finally rinsed again in 1 mL of ultrapure water.

Multi-parametric-surface plasmon resonance (MP-SPR) measurements. MP-SPR measurements were simultaneously performed at room temperature in both flow channels, at the wavelengths of 670 and 785 nm, with a MP-SPR Navi™ 200 OTSO instrument (BioNavis Ltd., Ylöjärvi, Finland). The intensity of the reflected light was measured at a resonant angle between 40 ° and 78 ° and all dual-wavelength SPR experiments were processed using the BioNavis Data viewer software.

Atomic Force Microscopy (AFM). AFM was used to investigate the surface morphology of the deposited liposomes on a solid surface. Measurements were carried out using Atomic Force Microscopy (AFM) operating in tapping mode (Nano-Observer AFM Microscope – CSInstrument.eu, Les Ulis, France). A liposome concentration of 1×10^{14} lipo/mL in PBS buffer (pH 4.5) was directly adsorbed on the cleaned SPR gold chip and on the streptavidin-functionalized SPR gold chip for 4 min at a flow rate of 50 µL/min and the excess of liposomes was subsequently washed. The chip was removed from the MP-SPR instrument, and about 1 mL of PBS buffer (pH 4.5) was gently deposited on the surface to prevent drying during AFM analysis. Topographic images were taken using AppNano Fort A tips with a normal spring constant of 0.6 - 3.7 N/m and a frequency of 30 kHz in liquid medium. Topographic images were generated at different positions of each sample. AFM images were treated with the free software Gwyddion.

Analysis of E4-GGYC interaction with immobilized liposomes. The interaction between E4-GGYC and immobilized liposomes was assessed using the MP-SPR method. After inserting the SPR gold chips functionalized with streptavidin into the BioNavis system, a continuous flow (50 µL/min) of PBS at pH 4.5 or pH 8 was firstly injected for approximately 20 min until a stable baseline was reached. After stabilization of the signal intensity, a liposome concentration of 1×10^{14} lipo/mL in PBS at pH 4.5 or pH 8 was injected on the streptavidin surface in both flow channels for 4 min at a flow rate of 50 µL/min. The liposome layer thereby formed on the

surface was then used as a model cell membrane surface to study the interaction with E4-GGYC. Peptide solutions were prepared immediately before injection by diluting the E4-GGYC mother solution in the desired volume of PBS buffer.

A peptide concentration range of 5-100 µM was injected onto the liposome layer. Initial concentrations of 5, 10, and 25 µM were injected for 4 min at a flow rate of 50 µL/min onto a newly prepared liposome-functionalized chip. High concentrations of 50, 75 and 100 µM were successively injected in a serial configuration onto the same liposome-functionalized chip for 4 min at a flow rate of 50 µL/min.

Each injection was followed by a washing step with the PBS buffer at 50 µL/min until the signal was stabilized to obtain a new baseline before another injection could be done. As the liposomes were immobilized on two flow cells, one was used for sample injection and the other was used to inject PBS buffer as reference. The MP-SPR signals vs. time at different E4-GGYC concentrations were recorded. Measurements were triplicated for each E4-GGYC concentration.

Kinetic study of the binding. In order to evaluate the immobilization of liposomes and the binding of E4-GGYC to liposomes, Trace Drawer™ for SPR Navi™ software was used to calculate kinetic parameters and affinity constants. For the calculations, the resulting sensorgrams were extracted via the SPR Navi™ Data viewer software and the dissociation constants (K_D) were calculated.

Biophysical analysis by MP-SPR. The SPR software Navi LayerSolver™ v. 1.2.1 (BioNavis Ltd., Ylöjärvi, Finland), provided as software associated with the MP-SPR instrument, employs the Fresnel-layer matrix formalism[23] to determine the thickness (*d*) and refractive index (*n*) of thin layers for a variety of biological applications.[17-18, 24-25] In the LayerSolver™ analysis software, the reflection spectra calculated from the Fresnel multilayer equations for p-polarized light at both laser wavelengths (670 and 785 nm) were fitted to the experimental SPR reflection

spectra to simultaneously determine *d* and *n* of the layer at the same time and at the same point.[17,23] Each layer was treated as an optically homogeneous and independent layer, and characterized by its thickness (*d*) and its complex refractive index ($\tilde{n}$) [26] defined by equation 1:

$\tilde{n} = n + ik$ (1)

where *n* is the real part of the complex refractive index that corresponds to the refraction of light and *k* is the imaginary part corresponding to the absorption of light by the layer.

An algorithm-based dual-wavelength method was used in this work to calculate the optical parameters of the multilayer system. The thickness value (*d*) was defined as a global variable for both wavelengths, whereas the complex refractive index was considered as an independent variable for the metal layer modeling ($k \neq 0$) and as a linearly dependent variable between the two wavelengths used for the other organic layers that do not absorb light ($k = 0$). The refractive index of the layer for the second wavelength, $n_{\lambda 2}$, was calculated using equation 2.

$$n_{\lambda 2} = n_{\lambda 1} + \frac{\mathrm{d}n}{\mathrm{d}\lambda} \times (\lambda 2 - \lambda 1) \quad (2)$$

Mono-rhamnolipid interaction with immobilized liposomes. The same protocol as previously described was used to prepare a liposome layer immobilized on a streptavidin-functionalized gold chip passivated with TRIS. The signal was stabilized for 4 min at a flow rate of 50 µL/min in PBS (pH 4.5). Then, a solution of 25 µM E4-GGYC in PBS pH 4.5 was injected at a flow rate of 12 µL/min for 15 min in channel 1, and in parallel, PBS pH 4.5 was injected at a flow rate of 12 µL/min for 15 min in channel 2. Then, a solution of 50 µg/mL mono-RL in PBS pH 4.5 was injected at a flow rate of 50 µL/min for 4 min. The SPR signal was measured at 670 and 785 nm.

RESULTS AND DISCUSSION

Physicochemical characterization of liposome samples. Biotinylated liposomes were prepared to develop the biomimetic model membrane. Dynamic light scattering (DLS) was used

to measure their mean hydrodynamic diameter and the polydispersity index (*PdI*) in 0.15 M NaCl solution, and in PBS at pH 4.5 and pH 8. The zeta potential of the liposomes was measured on the basis of their electrophoretic mobility. The physicochemical characterizations are given in Table 1.

Table 1. Characterization of liposomes. The average hydrodynamic diameters and zeta potentials are given as mean values ± standard error of the mean (*sem*) of three independent measurements. The *sem* was calculated with equation (S1) (see section 1 in supporting information).

Sample	Diameter (nm)	*PdI* [a]	Zeta potential (mV)	C_p [b] (mM)	C_l [c] (lipo/mL)	*RI* [d]
Liposomes/0.15 M NaCl solution	94 ± 3.7	0.14	−6.6 ±0.8	31	1.94×10^{14}	1.338
Liposomes/PBS pH 4.5	98 ± 1.1	0.15	−2.1 ± 0.5	31	1.80×10^{14}	1.334
Liposomes/PBS pH 8	99.6 ± 1.2	0.14	−4.0 ± 0.6	31	1.73×10^{14}	1.336

[a] Polydispersity index, [b] Concentration of phospholipids, [c] Concentration of liposomes, [d] Refractive index

In the different solutions, the liposomes presented an average size smaller than half the value of both wavelengths used in the MP-SPR device, so the SPR evanescent field could penetrate the entire liposome layer. The zeta potential values remained slightly negative in the different pHs due to the low amount of anionic biotinylated lipid (DSPE-PEG) in the composition. It can be noted that the global charge of the liposomes was low because the main lipid, phosphatidylcholine (HSPC), is zwitterionic. The liposomes maintained their hydrodynamic diameters as well as their negative zeta potential in solution over a period of 6 months ensuring an efficient electrostatic repulsion between them, which prevents their aggregation. Each

liposome suspension was carefully controlled for liposome size and ζ-potential before each MP-SPR experiment.

Measurement of the equilibrium dissociation constant K_D of liposome interaction with the functionalized surfaces. The gold surfaces were modified with different self-assembled monolayers (SAMs) of functional α,ω-alkanethiols with varying terminal groups (–CH_3, –COOH, and –NH_2) or with a streptavidin layer, following protocols described in a previous work.[19] Then, liposome immobilization on these surfaces was studied by recording the SPR signal upon injection of different concentrations of the liposome suspension. The binding affinity was assessed by the shift of the SPR angle position θ_{SPR} resulting from the change of refractive index induced by liposome binding. The association (k_a), dissociation (k_d) rate constants and equilibrium dissociation constants K_D of the interaction between biotinylated liposomes and the –CH_3, –COOH, –NH_2 (see Figure S2 and S3 in supporting information) and streptavidin (Figure S4) functionalized surfaces were calculated from the different sensorgrams, and displayed in Table 2 (See supporting information in section 3).

Table 2. Binding affinity of liposomes with different functionalized gold surfaces. The association (k_a), dissociation (k_d) rate constants and equilibrium dissociation constants (K_D), expressed as molar concentrations of phospholipids, were obtained from the fitting of the sensorgrams extracted with MP-SPR Navi Data viewer. K_D were calculated using the "Affinity" model for (–CH_3, –COOH, –NH_2) surfaces and the "OneToOne" model for the streptavidin surface. k_a and k_d were calculated using the "OneToOne" model.

Surface	k_a $(1/\mathrm{M} \times \mathrm{s})$	k_d $(1/\mathrm{s})$	K_D (M)
$-CH_3$	1.14×10^1	8.99×10^{-3}	7.20×10^{-4}
	$\pm 8.67 \times 10^{-1}$	$\pm 9.06 \times 10^{-5}$	$\pm 1.01 \times 10^{-4}$
$-COOH$	5.58×10^1	7.12×10^{-3}	1.09×10^{-4}
	$\pm 1.08 \times 10^1$	$\pm 2.94 \times 10^{-4}$	$\pm 0.74 \times 10^{-4}$

$-NH_2$	1.67×10^2 $\pm 9.02 \times 10^1$	3.64×10^{-3} $\pm 8.94 \times 10^{-5}$	2.06×10^{-5} $\pm 1.20 \times 10^{-5}$
Streptavidin	7.34×10^2 $\pm 1.43 \times 10^1$	6.92×10^{-9} $\pm 3.31 \times 10^{-5}$	9.44×10^{-12} $\pm 1.02 \times 10^{-12}$

The results show decreasing dissociation constants K_D corresponding to the increasing affinity of liposomes to the functionalized surface. The affinity increases following the order CH_3 < COOH < NH_2 < streptavidin. The interaction with CH_3, COOH and NH_2 surfaces were driven by either hydrophobic or electrostatic interactions as described in the literature [19,27] whereas liposome anchoring on the streptavidin layer showed a very strong affinity resulting from the presence of biotin on the liposome surface. The K_D for streptavidin is of the same order of magnitude as that of biotin-streptavidin affinity constant.[28-29] The latter protocol was selected to elaborate a highly stable liposome-functionalized surface to study the E4-GGYC interaction via MP-SPR.

As a preliminary experiment, the possible unspecific adsorption of the peptide on the streptavidin layer was checked by injection of a 10 μM peptide solution on the streptavidin-functionalized surface that has been passivated by either 10 mM of an aqueous solution of either tris(hydroxymethyl)aminomethane (TRIS), 3-dimethylaminopropylamine (DMAP), or lysine for 30 min. The peptide was injected in PBS buffer (pH 4.5) for 4 min, followed by a washing step in PBS at pH 4.5 (see Figure S5 in the supporting information). E4-GGYC adsorption on the streptavidin surface passivated with both DMAP and lysine generated a significant increase of the SPR signal, with $\Delta\theta_{SPR}$ of ca. 0.73 ° and 0.53 ° respectively. Conversely, a negligibly small signal was obtained with the TRIS-passivated surface, indicating a very low degree of unspecific binding. The TRIS protocol was selected to passivate surfaces functionalized with liposomes. It can be mentioned that after this complete functionalization protocol, the risk of

direct reaction of the cysteine of E4-GGYC on the gold surface covered by the successive layers of organic molecules is avoided.

Biotinylated liposomes were deposited on the streptavidin-covered SPR gold chip at a concentration of 1×10^{14} lipo/mL in PBS buffers at pH 4.5 and pH 8. Successful immobilization of the liposome was evidenced by first recording the full SPR angular spectrum. Injection of liposomes at both pHs resulted in fast deposition and generated a significant shift in the SPR angular peak minimum of ca. 1.80 ° and 1.75 ° at pH 4.5 and pH 8 respectively, compared to the streptavidin layer (Figure S6). The thickness values of the deposited liposome layer at both pHs, before and after rinsing with PBS, and calculated from the fitting of the corresponding SPR curves with LayerSolver^{TM} Software did not show any significant difference. An average thickness of d = 83 nm and d = 93 nm, and a refractive index of n = 1.3499 and n = 1.3446 of the liposome layer were obtained at pH 4.5 and pH 8 respectively.

The morphology of the streptavidin surface coated with liposomes was characterized by AFM in order to highlight the quality of liposome deposition. Liposomes are challenging objects to image by AFM due to their tendency to collapse during observations because of interactions with the tip.[30-33] As a reference, the gold surface roughness was measured through its root mean square roughness (RMS ≅ 1.53 nm for images of 2.5×2.5 µm^2 area) (see Figure S7 in the supporting information).

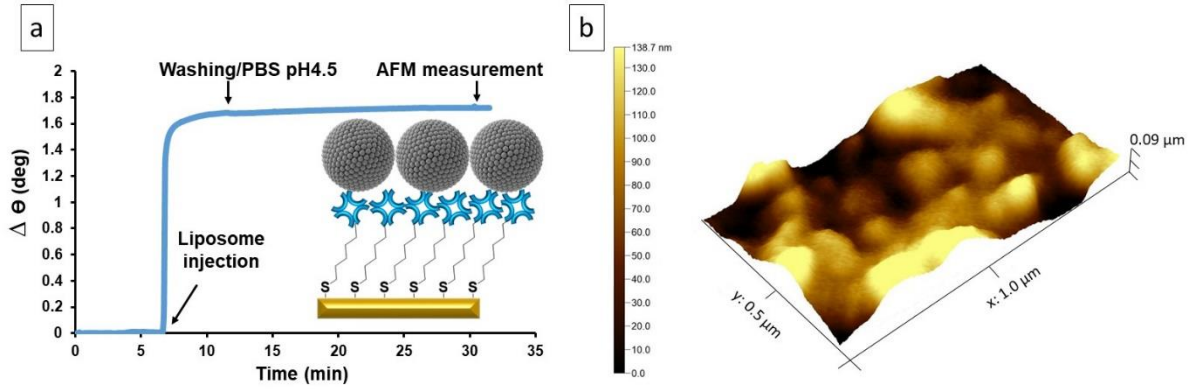

Figure 1. MP-SPR sensorgram of the liposome adsorption on a streptavidin functionalized surface before AFM measurement (a), and AFM topographic image by tapping-mode of the liposome-functionalized surface (b).

The AFM image of liposomes deposited on the streptavidin-functionalized gold surface shows a strong covering of the surface by globular objects (Figure 1). We observed a granulated surface, covered by intact liposomes with an average height slightly greater than 70 nm, close to the mean diameter of liposomes in aqueous suspension. The covering was formed by a monolayer of liposomes, lighter areas of the image may correspond to larger liposomes. These results showed that the biotin–streptavidin interaction promoted the adhesion of a dense layer of liposomes without changing their shape. This result is in agreement with the AFM characterization of biotinylated liposomes interacting with a streptavidin-functionalized glass surface reported by Takechi-Haraya *et al.* [33] showing that the shape of the liposomes was not impacted by their immobilization.

MP-SPR analysis of peptide interaction with the model membrane. The interaction of E4-GGYC with liposome-coated surface was investigated by recording full SPR angular spectra as a function of time. 5, 10 and 25 µM peptide solutions in PBS pH4.5 were injected at a constant flow rate of 50 µL/min.

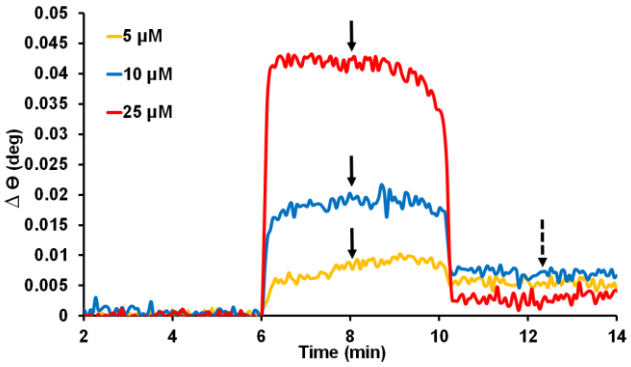

Figure 2. Superimposed sensorgrams (normalized peak angular position vs time) recorded during injection of 5–25 µM E4-GGYC peptide at pH 4.5 on the liposome-functionalized surface. The arrows indicate the positioning for *d* and *n* calculations (Table 3) at 670 nm.

Figure 2 shows that the interaction of the peptide with the liposome layer induced an increase in the SPR signal at pH 4.5. This increase was related to the concentration of peptide during the injection. It is worth noting that the injection of 10 µM of peptide at pH 4.5 resulted in an angle change of approximately + 0.02 °, whereas no significant change in the SPR angle was measured when the same concentration was allowed to interact with only the streptavidin layer passivated with TRIS (see Figure S5 in the supporting information). This confirmed that the signal variation measured during peptide interaction with the liposome layer reflects the actual peptide-liposome interaction and not peptide-streptavidin interaction.

Most notably, the sensorgrams indicate that the peptide/liposome association process is rapid, and reaches a stable state during the peptide injection. This suggests that the peptide is adsorbed onto or inserted into the lipid bilayer of liposomes during the injection period. Relative reversibility of the interaction was observed when the injection solution was changed to PBS solution at pH 4.5.

Figure 3 shows the measured and fitted SPR curves from real-time experiments after each injection of peptide onto the liposome layer at pH 4.5. The main SPR peak angular position shifted to higher angles with the addition of increasing concentrations of peptide at pH 4.5. The

curves were fitted separately with LayerSolver™ software, by considering each layer as a single optically homogeneous layer. The fit of this model to the experimental data was very good.

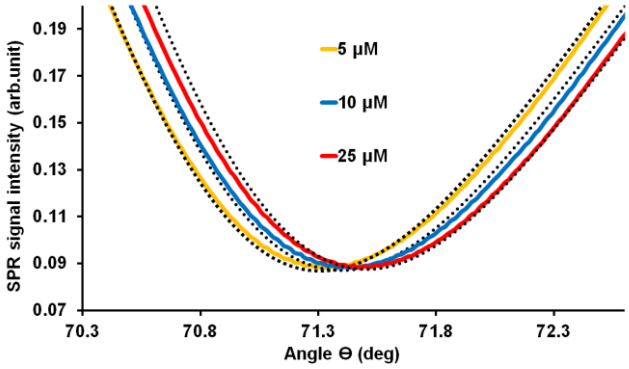

Figure 3. SPR peak full angle scans measured at 670 nm of the liposome-supported surfaces after injection of 5–25 µM E4-GGYC solutions at pH 4.5 (solid curves), with corresponding fits from LayerSolver™ modeling (dotted curves). The SPR curve corresponding to each concentration was taken at the equilibrium of peptide/liposome interaction for the modeling by LayerSolver™ software.

The modeling was started by determining the optical properties of the layers constituting the functionalized SPR gold chip, such as the chromium 'Cr' adhesion layer and the gold 'Au' layer of the cleaned SPR gold chip, as well as the two organic deposited layers of MUA and streptavidin. These calculations were based on the stepwise numerical iteration procedure in LayerSolver™, where the previous layer acted as a background to solve the optical parameters of the next layer.[19] The obtained parameters were maintained fixed and used as a basis for calculating the optical thickness (*d*) and the real refractive index (*n*) of the deposited liposome layer before and after injection of the different peptide concentrations.

The experiments were performed maintaining the same buffer for i) liposome deposition, ii) E4-GGYC binding, and iii) washing step to minimize the variation in refractive index caused by the buffer and to facilitate the interpretation of the experimental data.

According to the calculation, the addition of liposomes in PBS to the streptavidin surface generated a layer with an average thickness of d = 83 nm and a refractive index of n = 1.34997 at pH 4.5. The refractive index values of the liposome layer give an indication of the lipid/buffer ratio in the liposomes. The refractive index of the phospholipid reported in the literature was around 1.435–1.450,[34] while that of PBS was of 1.3352 at pH 4.5 (experimental data).

The resulting SPR curves in Figure S6 (blue curves) showed full SPR angular spectra without the formation of a waveguide peak in the vicinity of the total internal reflection (TIR) angle.[17,26] This was due to the fact that the liposome thickness formed on the surface was well below the penetration depth of the evanescent field (< 1/2 λ_1 and 1/2 λ_2). In this case, the SPR evanescent field allowed the detection of extremely small optical changes in the liposome layer during interaction with peptides. The variation of thickness (d) and refractive index (n) of the liposome layer during interaction with E4-GGYC were calculated from SPR LayerSolver™ simulations. Data are presented in Table 3. Figure 4a-b illustrate, in graph form, the variation of the calculated optical parameters (d and n) for the liposome layer as a function of injected peptide concentration at pH 4.5. The modeling was performed before and after the washing step with PBS.

Table 3. Thickness (*d, nm*), refractive index (*n, RIU*) of the liposome layer as well as the phospholipid concentration (*Cp, g/cm*^{3}) after each E4-GGYC injection (5-25 µM) and after each washing with PBS at pH4.5. The values represent the average (± standard deviation) of three independent calculations by the SPR LayerSolver™ simulation.

Peptide concentration (µM)	During peptide injection	Washing with PBS pH4.5
5	d = 86.62 ± 1.00	d = 84.03 ± 0.98
	n = 1.34041 ± 0.00120	n = 1.34381 ± 0.00100
	Cp=0.08585 ± 0.00265	Cp=0.08849 ± 0.00072

10	d = 92.05 ± 0.70	d= 86.06 ± 0.80
	n= 1.33974 ± 0.00050	n = 1.34200 ± 0.00150
	Cp=0.08078 ± 0.00045	Cp=0.08641 ± 0.00133
25	d = 93.70 ± 0.90	d = 86.27 ± 1.10
	n= 1.33886 ± 0.00100	n= 1.34030 ± 0.00080
	Cp=0.07936 ± 0.00152	Cp=0.08620 ± 0.00121

Pure liposome layer; d= 83.30 nm, n=1.34997, Cp=0.08925 g/cm^3

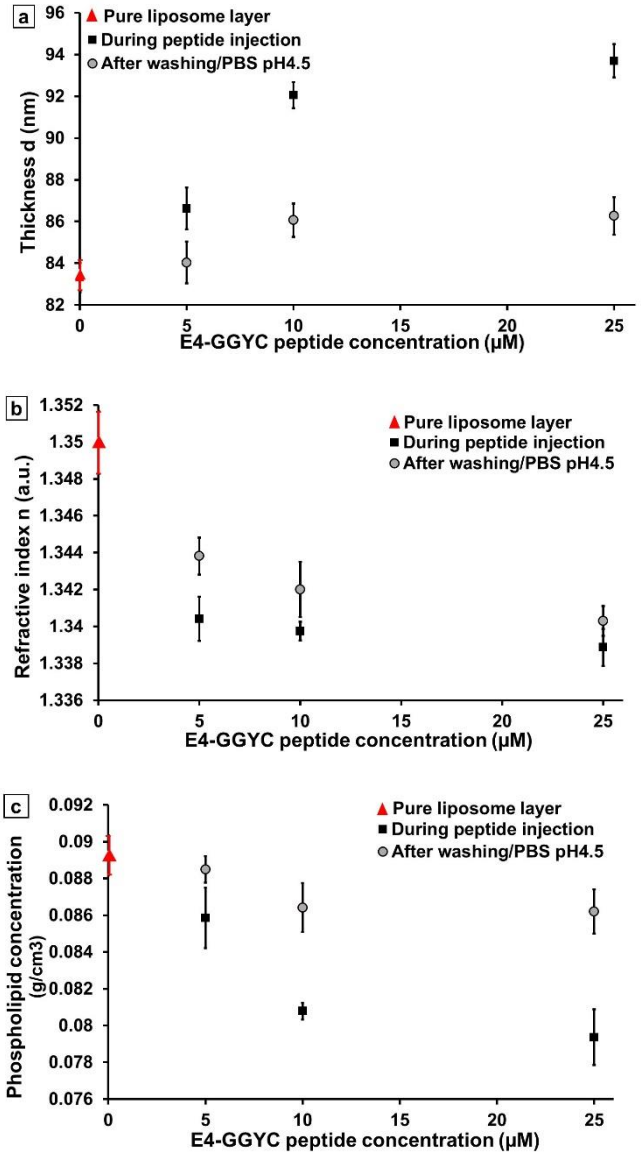

Figure 4. Effect of 5-25 µM E4-GGYC injection on the thickness *d* (a), refractive index *n* (b) and concentration of phospholipids *Cp* (c) of the immobilized liposome layer at pH 4.5, before and after the washing step in PBS, pH 4.5.

Figures 4.a shows that the liposome layer thickness increases from 83.3 nm to 93.7 nm upon addition of the peptide at pH 4.5 (data reported in Table 3). This progressive increase in thickness is accompanied by a decrease in the refractive index (*n*) from 1.34997 to 1.33886 (refractive index of the layer after 25 µM peptide injection) as shown in Figure 4b.

The angular shift in SPR peak minimum of an optically homogeneous layer according to the well-established Jung model [35] is proportional to *d* and *n* via equation 3.

$$\Delta\theta_{SPR} = S(n_L - n_b)[1 - e^{\left(-\frac{d}{\delta}\right)}] \qquad (3)$$

where *S* is the sensitivity factor per refractive index unit (deg), n_b and n_L are the bulk and layer refractive indices respectively, δ is the decay length of the intensity of the evanescent electric field and *d* is the thickness of the layer.

On the basis of this equation, it is clear from the simulated curves that the SPR response was mainly induced by the variation of the layer thickness (*d*). The multiple parameters extracted from simulated fits of the full SPR angular spectra measured in real-time during peptide-liposome interactions provide a means to explain the origin of the SPR response.

Thanks to the theoretical calculation, we were able to estimate the concentration of phospholipids (*Cp*) in the initial liposome layer as well as its variation due to E4-GGYC injection (Figure 4.c). This calculation was achieved in order to better understand the peptide effect on the liposome layer. The concentration of phospholipids in the initial liposome layer (before peptide injection) was calculated using equation (S5) provided by Feijter's formula. The resulting phospholipid concentration in the liposome layer after each peptide injection was calculated by considering that the increase in calculated thickness *d* was an increase in volume

of the liposome layer, and thus a change in phospholipid concentration. The *Cp* values calculated after the injection of 5–25 µM peptide using equation (S6) are presented in Table 3. Hence, *Cp* was estimated at 0.08925 g/cm^3 for the initial liposome layer. The concentration decreased in the presence of peptide, down to *Cp* ~ 0.07936 g/cm^3 at 25 µM peptide injection. Thus, we could hypothesize that during the injection of 5–25 µM peptide at pH 4.5, it penetrates the liposome membrane, probably causing the formation of pores in the membrane as described in the literature,[6] followed by the swelling of the liposomes by buffer flux. This leads on the one hand to an increase in the thickness due to the swelling and on the other hand, to a decrease in the refractive index of the layer induced by a larger volume of buffer inside the liposomes, which also explains the decrease in phospholipid concentration. Upon switching the medium to buffer (washing step), the calculated values of thickness, refractive index as well as phospholipid concentration proved that the swelling stopped and the peptide desorbed. The calculated values suggested a partial deflation of the liposome layer without perfectly returning to the initial values of the native layer.

In our case, we were unable to confirm the complete reversibility of the peptide insertion into the membrane as was previously shown by Longo *et al.* [36-37] and Zhelev *et al.* [6] Longo *et al.* showed that the Influenza fusion peptide (wt-20 HA2 peptide) rapidly inserts in the membrane at low pH and that insertion was mainly reversed by rinsing the membrane with buffer. Zhelev *et al*. studied the interaction of the HA2 peptide analog (AcE4K) with phosphatidylcholine liposomes and proved that the binding of the peptide increases as the pH decreases to pH 4.5, and the insertion proved to be reversible. They also observed that the peptide insertion in the lipidic membrane does not affect the membrane permeability for water, which shows that the peptide at concentrations ≤ 10 µM does not substantially perturb the packing of the hydrocarbon region. However, the ability of the membrane to retain solutes in the presence of peptide proved to be compromised, suggesting that the inserted peptide promotes the formation of short-lived

pores. This point was confirmed by our theoretical calculations when the refractive index *n* of the liposome layer decreased following the injection of 5–25 µM peptides at pH 4.5. We suggested that nanopores created by peptides upon insertion into the lipidic membrane facilitate the flux of buffer, which decreases the calculated concentration of phospholipids.

Kinetics of peptide interaction with liposomes at pH 4.5. The sensorgrams resulting from the E4-GGYC/liposome interactions at pH 4.5 were analyzed through Trace Drawer™ software to perform a kinetic study of the interactions. The fitting model adopted was the simple Langmuir binding, "one-to-one" reaction model (equation S3). The sensorgrams obtained at 5–25 µM peptide concentrations were fitted simultaneously to calculate the equilibrium dissociation constant (K_D). The binding mechanism described by this model is that of the peptide (P), which represents the analyte in solution, inserted in the immobilized liposome (L) as a ligand. During the process, the association (k_a) and dissociation (k_d) rate constants control the formation of the complex (PL) at the surface, as shown in equation 4.

$$P + L \Leftrightarrow PL \qquad (4)$$

Figure S8.a represents the overlay between experimental sensorgrams and fitted curves, while in Figure S8.b, the fitting residual values after subtraction from the experimental sensorgrams are shown. Satisfactory fits were obtained using the "OneToOne" binding model. The kinetic parameters obtained from the fitting are reported in Table 4. The peptide was inserted in the liposome membrane with a K_D of 4.5×10^{-7} M. This result was in good agreement with the K_D calculated by Rafalski *et al.* from fluorescence measurements of HA2 peptide binding to liposome vesicles ($K_D \sim 8 \times 10^{-7}$ M).[1]

Table 4. Kinetic parameters obtained from the fitting of the MP-SPR sensorgrams of E4-GGYC/liposome interaction. The values represent the average (± standard deviation) of three independent calculations by the "OneToOne" binding model.

	$k_a\ (10^5)(1/\mathrm{M}\times\mathrm{s})$	$k_d\ (10^{-1})(1/\mathrm{s})$	$K_D\ (10^{-7})(\mathrm{M})$
Peptide	2.820 ± 0.005	1.23000 ± 0.00006	4.50 ± 0.03

Effect of pH on peptide-lipid membrane interaction. We also studied the SPR response induced by the injection of peptide solutions at basic pH. Figure 5 shows the superimposed sensorgrams for 5-25 µM E4-GGYC injections at pH 4.5 and pH 8.

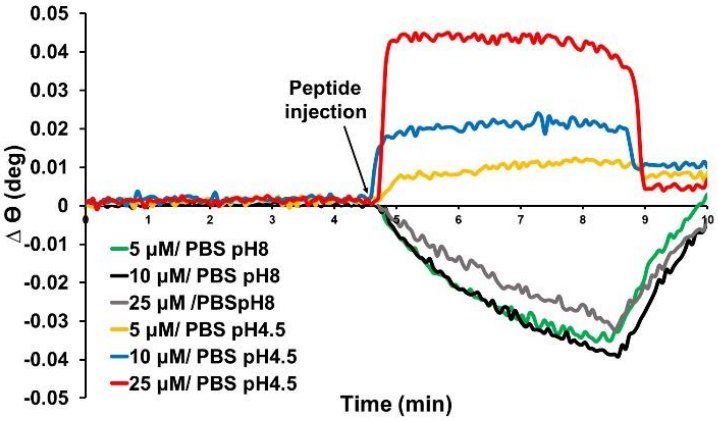

Figure 5. Superimposed sensorgrams of 5-25 µM E4-GGYC injections at pH 4.5 and pH 8 on the liposome-coated surface.

Sensorgrams revealed two different SPR responses, probably resulting from a different mechanism of interaction at both pHs. As a control, a study carried out in PBS at pH 4.5 and pH 8 confirmed that the SPR signal of the liposome-functionalized surface was stable upon pH variation.

Different binding kinetics in both association and dissociation rates were observed at pH 4.5 compared to pH 8. As shown, the same peptide concentrations injected at pH 8 led to a slow decrease in the signals regardless of the concentration used. The interaction kinetics were much slower than those observed at pH 4.5, and did not reach a stable signal within the injection time of 4 min. However, when the liposomes were rinsed with PBS (pH 8), the SPR angle started to increase again and about 4 min were required to reach the baseline.

Shifts in SPR signals were clearly concentration dependent for the peptide at pH 4.5, but not for pH 8, for which the variations in the SPR angles were similar for all concentrations tested. These results indicate that E4-GGYC has different modes of interaction with liposomes when moving from acidic to basic pH.

The negative shift in the SPR angle probably originates from morphological changes in the liposome monolayer. This suggests that injected peptide at basic pH probably induces a contraction of the liposomes accompanied by a return to their initial shape after rinsing. A similar behavior was shown by the studies of Viitala *et al.* [26] Cuerrier *et al.* [38] and Chabot *et al.* [39] Viitala *et al.* reported from MP-SPR studies that the simulation of MDCKII cells with the D-mannitol and propranolol drugs resulted in a negative shift in the angular position of the SPR peak minimum during cell stimulation and this was induced by the contraction of the cells. Cuerrier *et al.* and Chabot *et al.* showed that morphological changes in cells, i.e. contraction of cells, induced a negative SPR shift in the reflection intensity measured at a fixed angle. The studies carried out by MP-SPR at pH 8 do not allow us to conclude on the absence of interaction between E4-GGYC and liposome in this buffer. It will therefore be interesting to relate these studies to the results obtained by DLS and NTA to clearly conclude on the pH-dependence of the E4-GGYC/liposome interaction.

Peptide effect on liposome size in solution. The size and the polydispersity index (*PdI*) of liposomes represent pertinent parameters for their characterization.[40] These parameters can provide information on their stability and, as such, can allow a qualitative assessment of their interaction with E4-GGYC in our study. Thus, synthesized liposomes were suspended in PBS at pH 4.5 and pH 8 and hydrodynamic diameters of 98 nm and 99.6 nm were recorded by DLS, respectively. These solutions were then incubated for 30 min at room temperature with increasing concentrations of E4-GGYC (from 0.5 to 10 µM) in PBS at both pHs. The evolution of the hydrodynamic diameter and the polydispersity index (*PdI*) of the liposomes was then

controlled by DLS and Nanosight (NTA) techniques (Figure 6). The results clearly demonstrated that increasing concentrations of E4-GGYC in PBS at pH 4.5 induced a rise in liposome size, whereas the *PdI* remained relatively low. This strongly suggested that 0.5–10 µM peptide didn't induce any liposome aggregation, or destruction. On the other hand, increasing concentrations of peptide from 0.5 to 10 µM in PBS at pH 8 did not promote any significant change in liposome size, as hydrodynamic diameters and *PdI* values remained almost stable. Nanoparticle-Tracking Analysis (NTA) experiments by NanoSight revealed the same behavior. The size of the liposomes measured by NTA increased as a function of peptide concentrations, between 0.5 and 10 µM at pH 4.5, without reaching a plateau as observed by DLS. The difference in size between the two pH values was smaller by NTA measurements. It is known that the DLS measurement of the average hydrodynamic diameter is more impacted by the presence of aggregates, in a very small amount, than the NTA measurement.[41] Nevertheless, both techniques confirmed the results obtained by MP-SPR and showed the different behavior of E4-GGYC towards liposomes at pH 4.5 and pH 8.

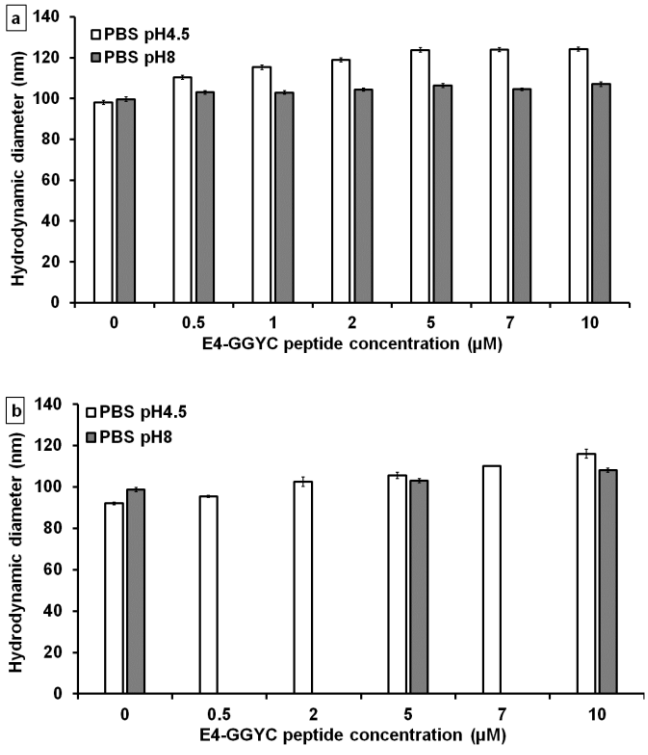

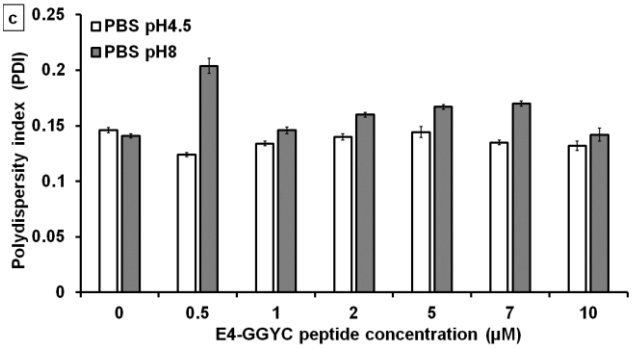

Figure 6. Effects of liposome incubation with increasing concentrations of E4-GGYC in PBS pH 4.5 and pH 8 on hydrodynamic diameter measured by DLS (a), NTA (b) and Polydispersity index (*PdI*) by DLS (c).

For the study, we were not able to increase the peptide concentration beyond 10 µM. Aggregates between peptides and liposomes were observed, which prevented us from obtaining interpretable data. This observation was in agreement with results reported by Zhelev *et al.*, who also described an aggregation of a similar peptide (AcE4K) at a concentration ≥ 10 µM and under pH < 6, in the presence of liposomes in solution. Whereas the aggregation of peptide was not observed by light scattering at 10 µM of a pure peptide solution, it precipitated from the solution only in the presence of liposomes when the pH was below 6.[6]

By these results, we confirmed the swelling process of liposomes at pH 4.5 by DLS and NTA, up to 10 µM of peptide in solution. For higher concentrations of peptide, peptide-liposome conjugates started to aggregate and precipitated, disturbing the DLS and NTA measurements, but not the MP-SPR response monitored on liposome-functionalized substrates. In the literature, the liposome swelling in a solution of 10 µM HA2 peptide was described by Zhelev *et al.* Similarly to our DLS results, they also confirmed that the peptide-liposome conjugates deteriorated with time in peptide solutions at concentration ≥ 10 µM. The authors then concluded that the lipid membrane was broken by a possible fusion process. Thanks to our results obtained by MP-SPR, we were able to monitor the peptide/liposome interaction up to

25µM peptide, showing a partial reversibility of the binding without disruption of the liposome layer.

Disruption assays of the supported liposome layer. In an attempt to destroy the liposome layer, we carried out the experiment with increasing peptide concentrations up to 100 µM. Figure 7.a shows the full real-time sensorgrams of the main SPR peak angular position for 50, 75 and 100 µM E4-GGYC at pH 4.5. With regard to the MP-SPR results, we were able to conclude that the interaction of E4-GGYC at pH 4.5 with the lipid layer up to 100 µM did not induce any perturbation of the membrane leading to the disruption of the liposomes. Indeed, we did not observe a drop in the SPR signal that could correspond to this degradation.

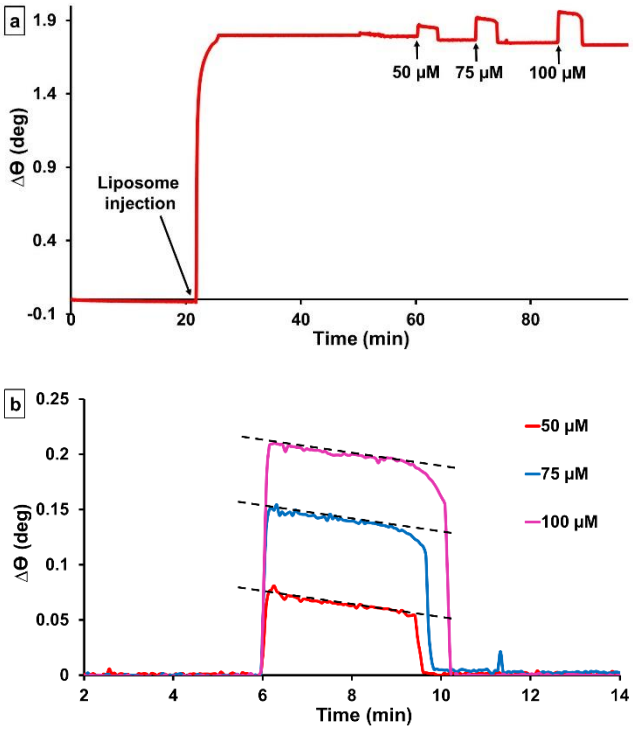

Figure 7. The full sensorgram (a) and the superimposed sensorgrams (b) measured at a wavelength of 670 nm, during the interaction 50-100µM E4-GGYC at pH 4.5 on immobilized liposomes.

Compared to Figure 2, the sensorgram in Figure 7.b revealed that E4-GGYC at acidic pH and at a concentration higher than 25 µM bound differently to the liposome surface. Here, the initial

peptide/liposome association mechanism was also rapid. But after that, the signal slowly decreased over time until the end of the peptide injection without reaching a steady state. Upon switching to PBS pH 4.5, a rapid drop in SPR signal to the baseline was recorded. Between small and high concentrations, we noticed that there was a probable transition in the mode of action of the peptide with the layer of liposomes. This observation was consistent with the shape of the sensorgram, showing a plateau of the signal during injection of 5-25 µM peptide (Figure 2), whereas a steady state was not observed during injection of 50-100µM peptide (Figure 7.b). This allows us to hypothesize that the peptide concentration of 25 µM was a critical concentration to saturate the membrane of the liposome layer. At 50-100 µM, the peptide first inserted into liposomes until saturation, then the excess peptide continued to adsorb onto the surface of the lipid layer, again causing an increase in the SPR signal related to peptide concentration.

Once a maximum amount of peptide was inserted and saturated the liposome membrane, the vesicular structure of the liposome was not destroyed. These results suggested that the insertion of E4-GGYC at pH 4.5 into the lipid bilayer increased the robustness of the liposome membrane. This point was experimentally investigated in the following experiment.

The stability of the lipidic membrane and its robustness were studied after the injection of 25 µM E4-GGYC on a liposome-functionalized chip. In a previous work, the rupture of liposomes by interaction with mono-rhamnolipid (mono-RL), a biosurfactant, was proven by MP-SPR.[19] Here, a solution of mono-RL was injected onto the liposome layer after the injection of peptide at pH 4.5, and in parallel onto a peptide-free liposome layer as a reference (Figure 8). The protocol was applied as described in the experimental part, i.e.: step (1) preparation of a liposome-functionalized substrate in PBS at pH 4.5, step (2) injection of 25 µM E4-GGYC in PBS at pH 4.5 (red curve), and in parallel, injection of PBS at pH 4.5 (blue curve), step (3) injection of mono-RL at a concentration of 50 µg/mL in the same phosphate buffer.

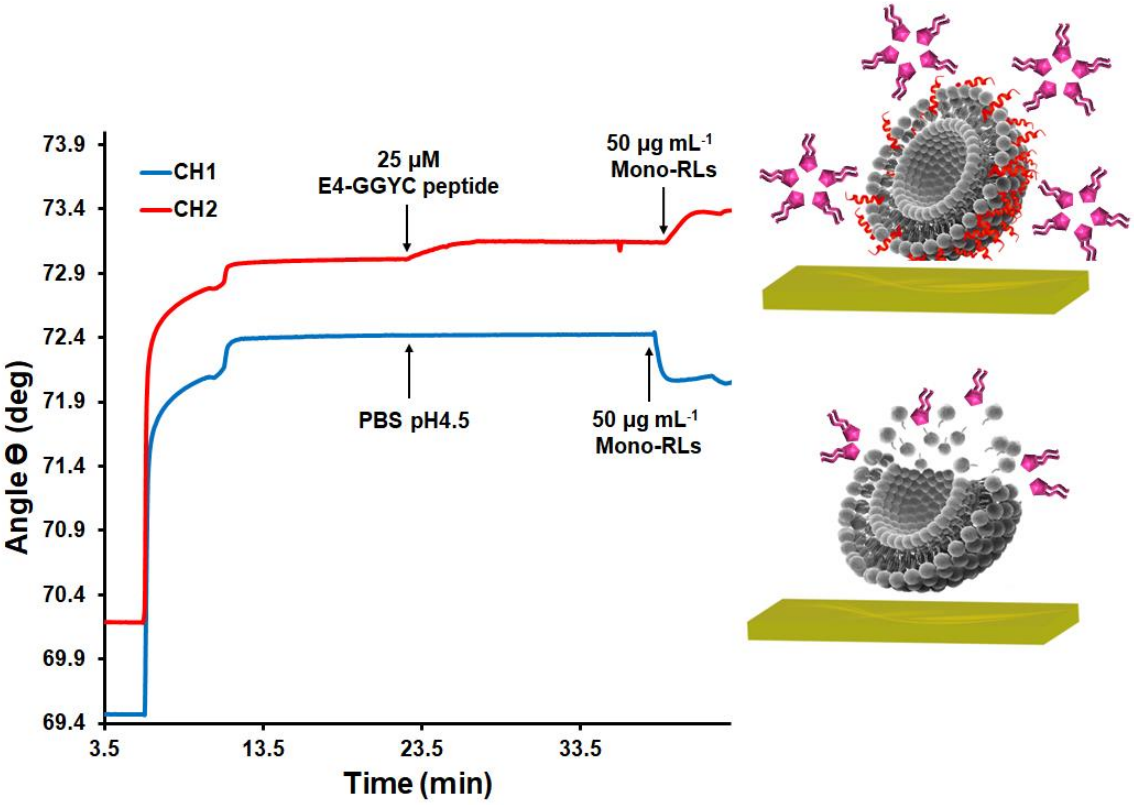

Figure 8. Sensorgrams measured in PBS pH 4.5 and at 670 nm wavelength during mono-RL injection at a concentration of 50 µg/mL on a pure liposome layer (CH1) and on a liposome layer saturated with 25 µM of E4-GGYC peptide at pH 4.5 (CH2) .

During E4-GGYC injection (Figure 8, red curve), we observed a progressive increase in the SPR angle, followed by a stabilization of the signal to a plateau. This variation was characteristic of peptide insertion into the lipid membrane. The subsequent step was the injection of mono-RL in order to study its interaction with the lipidic membrane. The addition of mono-RL led to a further increase in the SPR angle. Thus, the positive change in SPR angle was proportional to the amount of mono-RL deposited on the surface. By contrast, injection of mono-RL onto the peptide-free liposome layer resulted in a significant drop of the SPR signal, showing that mono-RL interacted with liposomes, and started to destroy them. The disruption of tethered liposomes by mono-RL has already been described by our group.[19] We reported that the liposome layer immobilized on a support could be disrupted and restructured with loss of

phospholipid material by the action of mono-RL. A clear drop in the SPR signal was observed and optical parameters (*d* and *n*) calculated by MP-SPR confirmed the formation of the phospholipid bilayer after complete degradation.[19] Likewise, Bombard *et al.* described the disruption of a liposome-supported surface by an amphiphilic peptide (AH peptide from the Hepatitis C virus) using Surface Plasmon Resonance Imaging (SPRi) and BALM technique. They recorded an increase in SPRi signal (reflectivity) just after injection of the fusogenic peptide onto the liposome layer, indicating liposome swelling, and afterwards a remarkable signal drop, reflecting lipid material loss and liposome disruption.

Our results confirmed that the presence of E4-GGYC inserted in the double lipid layer of liposomes inhibited mono-RL-triggered disruption by enhancing membrane robustness. In the literature, a number of studies have shown that the HA2 peptide intercalates in the outer leaflet of the lipid bilayer, increasing the ordering in the head groups of this layer, and thus increasing its robustness. [42-44] Furthermore, studies revealed that the peptide does not cross the double phospholipid layer and remains positioned in the outer part of the membrane.[43] It has been described that the coupling between the hardened outer leaflet due to peptide insertion and the softer inner leaflet generates bending stresses in the bilayer. The authors suggested that these stresses may initiate the membrane fusion. In our case, the results obtained by SPR on a layer of supported liposomes did not allow us to observe the fusion mechanism up to 100µM peptide in solution.

CONCLUSION

The interaction of E4-GGYC, an analog of HA2 peptide of Influenza virus hemagglutinin, with a biomimetic surface formed with liposomes grafted on a gold substrate was studied by the MP-SPR method. A biotin/streptavidin binding strategy was developed to create a stable layer of liposomes with high coverage, as characterized by AFM. The SPR signal variation clearly

illustrated the strong binding of the biotinylated liposomes to the streptavidin-functionalized surface with a calculated K_D of 9.44 10^{-12} M. We demonstrated the capacity of the MP-SPR technique to characterize the variation of the liposome layer morphology upon injection of E4-GGYC at pH 4.5 and pH 8 and we revealed different interaction mechanisms. At pH 4.5, the peptide first inserted into the liposome membrane to saturation, and then adsorbed on the surface at high concentration, whereas the interaction mechanism did not follow the same mechanism at pH 8. The negative shift in the SPR angle observed upon peptide injection at pH 8 probably originated from morphological changes in the liposome layer. The binding sensorgrams of 5–25 µM peptide with the liposome layer at pH 4.5 were fitted to calculate an equilibrium dissociation constant K_D of 4.50 10^{-7} M. In our study, MP-SPR studies showed that liposomes swelled in the presence of peptides in the circulating solution at pH 4.5. This assumption was proven theoretically by calculating the thickness (*d*) and refractive index (*n*) of the liposome layer by the SPR Navi LayerSolver^{TM} software. This pH-dependent swelling was confirmed in solution by Dynamic Light Scattering (DLS) and a NanoSight Nanoparticle-Tracking Analysis (NTA). High concentrations of peptide up to 100 µM did not break down the structure of the liposomes grafted on the surface. Our studies also revealed that peptide insertion increased the robustness of the lipid membrane. The well-known disruption mechanism by mono-rhamnolipids did not occur after peptide insertion into the liposome membrane. As a further conclusion, MP-SPR analyses of E4-GGYC peptide interaction with immobilized liposomes did not allow us to observe the fusion mechanism up to 100µM peptide in solution. In view of the studies presented here, we believe that our MP-SPR approach on liposomes immobilized on solid substrates can provide real-time complementary information for a better mechanistic understanding of biomolecule/lipid membrane interaction. The kinetic study of a complex interaction and the individual characterization of each surface modification step (changes in thickness and refractive index) are carried out using a single device. The

method makes it possible to study the mechanisms of interaction while avoiding the risk of precipitation of liposomes observed in solution. Within the broader scope of this work, we assume that the approach can be extremely interesting to study the mechanisms of action of the majority of cell-penetrating peptides whose therapeutic properties are of great interest. This work also opens promising perspectives for studying unknown interactions between a bi-lipidic membrane and entities of interest such as drugs, biosurfactants, peptides, proteins, antibodies or microorganisms.

ACKNOWLEDGEMENTS

The authors would like to thank the Tunisian government for financial support of Meryem Belkilani's PhD thesis. The authors also acknowledge Silvia BREUSA (University of Claude Bernard Lyon 1) for the NTA measurement.

SUPPORTING INFORMATION

Error parameter calculation; E4-GGYC characterization by HPLC; Experimental protocol, SPR sensorgrams and fitted curves of the interaction of liposomes with functionalized surfaces; passivation of the streptavidin-functionalized surface; full SPR angular spectra of the streptavidin-functionalized surface and the liposome-supported surface; AFM characterization of the gold surface; calculation of the phospholipid concentration in the liposome layer; fitting and subtraction of the fitted curves of peptide/liposome interaction.

ABBREVIATIONS

MP-SPR, Multi-parametric surface plasmon resonance; MUA, 11-mercaptoundecanoic acid; PBS, phosphate buffered saline; DLS, Dynamic Light Scattering; *PdI*, polydispersity index;

SAM, self-assembled monolayers; *SD*, standard deviation; θ_{SPR}, SPR angular peak minimum, Mono-RL, mono-rhamnolipid.

REFERENCES

(1) Rafalski, M.; Ortiz, A.; Rockwell, A.; Van Ginkel, L. C.; Lear, J. D.; DeGrado, W. F.; Wilschut, J. Membrane Fusion Activity of the Influenza Virus Hemagglutinin: Interaction of HA2 N-Terminal Peptides with Phospholipid Vesicles. *Biochemistry* **1991**, *30* (42), 10211–10220.

(2) Wagner, E.; Plank, C.; Zatloukal, K.; Cotten, M.; Birnstiel, M. L. Influenza Virus Hemagglutinin HA-2 N-Terminal Fusogenic Peptides Augment Gene Transfer by Transferrin-Polylysine-DNA Complexes: Toward a Synthetic Virus-like Gene-Transfer Vehicle. *Proc. Natl. Acad. Sci.* **1992**, *89* (17), 7934–7938.

(3) Chaix, C.; Pacard, E.; Elaïssari, A.; Hilaire, J.-F.; Pichot, C. Surface Functionalization of Oil-in-Water Nanoemulsion with a Reactive Copolymer: Colloidal Characterization and Peptide Immobilization. *Colloids Surf. B Biointerfaces* **2003**, *29* (1), 39–52.

(4) Skehel, J. J.; Cross, K.; Steinhauer, D.; Wiley, D. C. Influenza Fusion Peptides. *Biochem. Soc. Trans.* **2001**, *29* (4), 623–626.

(5) Russell, C. J. Orthomyxoviruses: Structure of Antigens. *Encyclopedia of Virology*, **2008**, 489-494.

(6) Zhelev, D. V.; Stoicheva, N.; Scherrer, P.; Needham, D. Interaction of Synthetic HA2 Influenza Fusion Peptide Analog with Model Membranes. *Biophys. J.* **2001**, *81* (1), 285–304.

(7) Lüneberg, J.; Martin, I.; Nüßler, F.; Ruysschaert, J. M.; & Herrmann, A. Structure and topology of the influenza virus fusion peptide in lipid bilayers. *J. Biol. Chem.* **1995**, *270* (46), 27606–27614.

(8) Vaccaro, L.; Cross, K. J.; Kleinjung, J.; Straus, S. K.; Thomas, D. J.; Wharton, S. A.; Skehel, J. J.; Fraternali, F. Plasticity of Influenza Haemagglutinin Fusion Peptides and Their Interaction with Lipid Bilayers. *Biophys. J.* **2005**, *88* (1), 25–36.

(9) Mozsolits, H.; Aguilar, M.-I. Surface Plasmon Resonance Spectroscopy: An Emerging Tool for the Study of Peptide–Membrane Interactions. *Pept. Sci. Orig. Res. Biomol.* **2002**, *66* (1), 3–18.

(10) Zhang, L.; Longo, M. L.; Stroeve, P. Mobile Phospholipid Bilayers Supported on a Polyion/Alkylthiol Layer Pair. *Langmuir* **2000**, *16* (11), 5093–5099.

(11) Luchini, A.; Tidemand, F. G.; Johansen, N. T.; Campana, M.; Sotres, J.; Ploug, M.; Cárdenas, M.; Arleth, L. Peptide Disc Mediated Control of Membrane Protein Orientation in Supported Lipid Bilayers for Surface-Sensitive Investigations. *Anal. Chem.* **2019**, *92* (1), 1081–1088.

(12) Hwang, B.; Ise, H. Multimeric Conformation of Type III Intermediate Filaments but Not the Filamentous Conformation Exhibits High Affinity to Lipid Bilayers. *Genes Cells* **2020**, *25* (6), 413–426.

(13) Skyttner, C.; Enander, K.; Aronsson, C.; Aili, D. Tuning Liposome Membrane Permeability by Competitive Coiled Coil Heterodimerization and Heterodimer Exchange. *Langmuir* **2018**, *34* (22), 6529–6537.

(14) Bompard, J.; Maniti, O.; Aboukhachfe, R.; Ausserre, D.; Girard-Egrot, A. BALM: Watching the Formation of Tethered Bilayer Lipid Membranes with Submicron Lateral Resolution. *Langmuir* **2021**, *37* (31), 9457–9471.

(15) Chadli, M.; Rebaud, S.; Maniti, O.; Tillier, B.; Cortès, S.; Girard-Egrot, A. New Tethered Phospholipid Bilayers Integrating Functional G-Protein-Coupled Receptor Membrane Proteins. *Langmuir* **2017**, *33* (39), 10385–10401.

(16) Parkkila, P.; Elderdfi, M.; Bunker, A.; Viitala, T. Biophysical Characterization of Supported Lipid Bilayers Using Parallel Dual-Wavelength Surface Plasmon Resonance and Quartz Crystal Microbalance Measurements. *Langmuir* **2018**, *34* (27), 8081–8091.

(17) Granqvist, N.; Liang, H.; Laurila, T.; Sadowski, J.; Yliperttula, M.; Viitala, T. Characterizing Ultrathin and Thick Organic Layers by Surface Plasmon Resonance Three-Wavelength and Waveguide Mode Analysis. *Langmuir* **2013**, *29* (27), 8561–8571.

(18) Kari, O. K.; Rojalin, T.; Salmaso, S.; Barattin, M.; Jarva, H.; Meri, S.; Yliperttula, M.; Viitala, T.; Urtti, A. Multi-Parametric Surface Plasmon Resonance Platform for Studying Liposome-Serum Interactions and Protein Corona Formation. *Drug Deliv. Transl. Res.* **2017**, *7* (2), 228–240.

(19) Belkilani, M.; Shokouhi, M.; Farre, C.; Chevalier, Y.; Minot, S.; Bessueille, F.; Abdelghani, A.; Jaffrezic-Renault, N.; Chaix, C. Surface Plasmon Resonance Monitoring of Mono-Rhamnolipid Interaction with Phospholipid-Based Liposomes. *Langmuir* **2021**, *37* (26), 7975–7985.

(20) Dua, J. S.; Rana, A. C.; Bhandari, A. K. Liposome: Methods of Preparation and Applications. *Int J Pharm Stud Res* **2012**, *3* (2), 14–20.

(21) Zhao, Y.; Du, D.; Lin, Y. Glucose Encapsulating Liposome for Signal Amplification for Quantitative Detection of Biomarkers with Glucometer Readout. *Biosens. Bioelectron.* **2015**, *72*, 348–354.

(22) Jakobsen, U.; Vogel, S. Assembly of Liposomes Controlled by Triple Helix Formation. *Bioconjug. Chem.* **2013**, *24* (9), 1485–1495.

(23) Albers, W. M.; Vikholm-Lundin, I. Surface plasmon resonance on nanoscale organic films. In *Nano-Bio-Sensing*; Springer: 2011; pp 83-125.

(24) Zacher, T.; Wischerhoff, E. Real-Time Two-Wavelength Surface Plasmon Resonance as a Tool for the Vertical Resolution of Binding Processes in Biosensing Hydrogels. *Langmuir* **2002**, *18* (5), 1748–1759.

(25) Zhou, M.; Otomo, A.; Yokoyama, S.; Mashiko, S. Estimation of Organic Molecular Film Structures Using Surface–Plasmon Resonance Spectroscopy. *Thin Solid Films* **2001**, *393* (1), 114–118.

(26) Viitala, T.; Granqvist, N.; Hallila, S.; Raviña, M.; Yliperttula, M. Elucidating the signal responses of multi-parametric surface plasmon resonance living cell sensing: a comparison between optical modeling and drug–MDCKII cell interaction measurements. *PloS one* **2013**, *8* (8), e72192.

(27) Fenzl, C.; Genslein, C.; Domonkos, C.; A. Edwards, K.; Hirsch, T.; J. Baeumner, A. Investigating Non-Specific Binding to Chemically Engineered Sensor Surfaces Using Liposomes as Models. *Analyst* **2016**, *141* (18), 5265–5273.

(28) Haes, A. J.; Van Duyne, R. P. A nanoscale optical biosensor: sensitivity and selectivity of an approach based on the localized surface plasmon resonance spectroscopy of triangular silver nanoparticles. *J. Am. Chem. Soc*. **2002**, *124* (35), 10596-10604.

(29) Kipriyanov, S. M.; Breitling, F.; Little, M.; Dübel, S. Single-Chain Antibody Streptavidin Fusions: Tetrameric Bifunctional ScFv-Complexes with Biotin Binding Activity and Enhanced Affinity to Antigen. *Hum. Antibodies* **1995**, *6* (3), 93–101.

(30) Sacconi, A.; Tadini-Buoninsegni, F.; Tiribilli, B.; Margheri, G. A Comparative Study of Phosphatidylcholine versus Phosphatidylserine-Based Solid Supported Membranes for the Preparation of Liposome-Rich Interfaces. *Langmuir* **2018**, *34* (40), 12183–12190.

(31) Viitala, T.; Hautala, J. T.; Vuorinen, J.; Wiedmer, S. K. Structure of Anionic Phospholipid Coatings on Silica by Dissipative Quartz Crystal Microbalance. *Langmuir* **2007**, *23* (2), 609–618.

(32) Kilic, A.; Kok, F. N. Biomimetic Lipid Bilayers on Solid Surfaces: Models for Biological Interactions. *Surf. Innov.* **2016**, *4* (3), 141–157.

(33) Takechi-Haraya, Y.; Goda, Y.; Izutsu, K.; Sakai-Kato, K. Improved Atomic Force Microscopy Stiffness Measurements of Nanoscale Liposomes by Cantilever Tip Shape Evaluation. *Anal. Chem.* **2019**, *91* (16), 10432–10440.

(34) Mashaghi, A.; Swann, M.; Popplewell, J.; Textor, M.; Reimhult, E. Optical anisotropy of supported lipid structures probed by waveguide spectroscopy and its application to study of supported lipid bilayer formation kinetics. *Anal. Chem*. **2008**, *80* (10), 3666-3676.

(35) Jung, L. S.; Campbell, C. T.; Chinowsky, T. M.; Mar, M. N.; Yee, S. S. Quantitative Interpretation of the Response of Surface Plasmon Resonance Sensors to Adsorbed Films. *Langmuir* **1998**, *14* (19), 5636–5648.

(36) Longo, M. L.; Waring, A. J.; Gordon, L. M.; Hammer, D. A. Area Expansion and Permeation of Phospholipid Membrane Bilayers by Influenza Fusion Peptides and Melittin. *Langmuir* **1998**, *14* (9), 2385–2395.

(37) Longo, M. L.; Waring, A. J.; Hammer, D. A. Interaction of the Influenza Hemagglutinin Fusion Peptide with Lipid Bilayers: Area Expansion and Permeation. *Biophys. J.* **1997**, *73* (3), 1430–1439.

(38) Cuerrier, C. M.; Chabot, V.; Vigneux, S.; Aimez, V.; Escher, E.; Gobeil, F.; Charette, P. G.; Grandbois, M. Surface Plasmon Resonance Monitoring of Cell Monolayer Integrity: Implication of Signaling Pathways Involved in Actin-Driven Morphological Remodeling. *Cell. Mol. Bioeng.* **2008**, *1* (4), 229–239.

(39) Chabot, V.; Cuerrier, C. M.; Escher, E.; Aimez, V.; Grandbois, M.; Charette, P. G. Biosensing Based on Surface Plasmon Resonance and Living Cells. *Biosens. Bioelectron.* **2009**, *24* (6), 1667–1673.

(40) Kanásová, M.; Nesměrák, K. Systematic Review of Liposomes' Characterization Methods. *Monatshefte Für Chem.-Chem. Mon.* **2017**, *148* (9), 1581–1593.

(41) Kim, A.; Ng, W. B.; Bernt, W.; Cho, N.-J. Validation of Size Estimation of Nanoparticle Tracking Analysis on Polydisperse Macromolecule Assembly. *Sci. Rep.* **2019**, *9* (1), 1–14.

(42) Ge, M.; Freed, J. H. Fusion Peptide from Influenza Hemagglutinin Increases Membrane Surface Order: An Electron-Spin Resonance Study. *Biophys. J.* **2009**, *96* (12), 4925–4934.

(43) Lai, A. L.; Freed, J. H. The Interaction between Influenza HA Fusion Peptide and Transmembrane Domain Affects Membrane Structure. *Biophys. J.* **2015**, *109* (12), 2523–2536.

(44) Lai, A. L.; Park, H.; White, J. M.; Tamm, L. K. Fusion Peptide of Influenza Hemagglutinin Requires a Fixed Angle Boomerang Structure for Activity. *J. Biol. Chem.* **2006**, *281* (9), 5760–5770.